



Structures of randomly generated mutants of T4 lysozyme show that protein stability can be enhanced by relaxation of strain and by improved hydrogen bonding via bound solvent

PHILIP PJURA¹ AND BRIAN W. MATTHEWS

Institute of Molecular Biology, Howard Hughes Medical Institute and Department of Physics,
University of Oregon, Eugene, Oregon 97403

(RECEIVED July 29, 1993; ACCEPTED September 16, 1993)

Abstract

The structures of three mutants of bacteriophage T4 lysozyme selected using a screen designed to identify thermostable variants are described. Each of the mutants has a substitution involving threonine. Two of the variants, Thr 26 → Ser (T26S) and Thr 151 → Ser (T151S), have increased reversible melting temperatures with respect to the wild-type protein. The third, Ala 93 → Thr (A93T), has essentially the same stability as wild type. Thr 26 is in the wall of the active-site cleft. Its replacement with serine results in the rearrangement of nearby residues, most notably Tyr 18, suggesting that the increase in stability may result from the removal of strain. Thr 151 in the wild-type structure is far from the active site and appears to sterically prevent the access of solvent to a preformed binding site. In the mutant, the removal of the methyl group allows access to the solvent binding site and, in addition, the Ser 151 hydroxyl rotates to a new position so that it also contributes to solvent binding. Residue 93 is in a highly exposed site on the surface of the molecule, and presumably is equally solvent exposed in the unfolded protein. It is, therefore, not surprising that the substitution Ala 93 → Thr does not change stability. The mutant structures show how chemically similar mutations can have different effects on both the structure and stability of the protein, depending on the structural context. The results also illustrate the power of random mutagenesis in obtaining variants with a desired phenotype. Although knowledge of the mutant structures makes it possible to rationalize their behavior, it would have been very difficult to predict in advance that these mutants would be stabilizing.

Keywords: mutagenesis; prediction; structural context; thermostability

The lysozyme from bacteriophage T4 is being used to help understand the interactions that contribute to protein stability (Matthews, 1987, 1993). One approach has been to design and construct mutants intended to increase protein thermostability. Such studies have confirmed that disulfide bridges (Matsumura et al., 1989), α -helix dipoles (Nicholson et al., 1991), changes in α -helix propensity (Zhang et al., 1991), and changes in entropy (Matthews et al., 1987) can all be effective. Another approach capable of revealing novel and perhaps unanticipated aspects of protein stability is the analysis of randomly generated mutants. Here we describe the structures of three mutant lysozymes that were selected using a screen designed to

identify thermostable variants (see Kinemage 1; Pjura et al., 1993). Two mutations, T26S and T151S, result in an increase of 0.9–1.3 °C in the reversible thermodynamic melting temperature relative to wild-type protein (WT*). The third, A93T, has essentially the same stability as the WT* (Table 1). Taken together, the variants represent three examples of the same type of amino acid substitution in the protein, but in entirely different structural

Table 1. Stability and activity of mutant lysozymes^a

	WT*	T26S	A93T	T151S
Change in melting temperature relative to wild type at pH 5.4 (°C)	0.0	1.35	0.13	0.93
Activity relative to WT* (%)	100	75	105	86

^a From Pjura et al. (1993).

Reprint requests to: Brian W. Matthews, Institute of Molecular Biology, Howard Hughes Medical Institute and Department of Physics, University of Oregon, Eugene, Oregon 97403.

¹ Present address: Department of Chemical Engineering, University of Delaware, Colburn Laboratory, Newark, Delaware 19716.

contexts. The structural changes associated with these mutations are described and discussed with respect to their thermodynamic consequences.

Results

T26S

Figure 1A shows the difference map in the vicinity of the mutation. A large negative difference peak at the position of Thr 26 $C\gamma^2$ indicates the loss of this methyl group in the mutant. Two smaller, positive and negative peaks near $O\gamma^1$ indicate that the side chain undergoes a small rota-

tion. In addition, the map shows large, correlated, positive and negative difference peaks near the side chain of Tyr 18, indicating a shift of the entire phenol ring toward the site of the lost methyl group.

Figure 2A compares the final, refined model for the mutant with the wild-type structure. It shows that a series of coordinated shifts of a number of residues in the N-terminal domain has occurred. Because of the loss of a close contact (2.9 Å) between the γ -methyl of Thr 26 and the hydroxyl group of Tyr 18, the entire tyrosine ring shifts toward residue 26. The motion of Tyr 18 brings with it the adjacent side chain of Arg 14, and the shift of

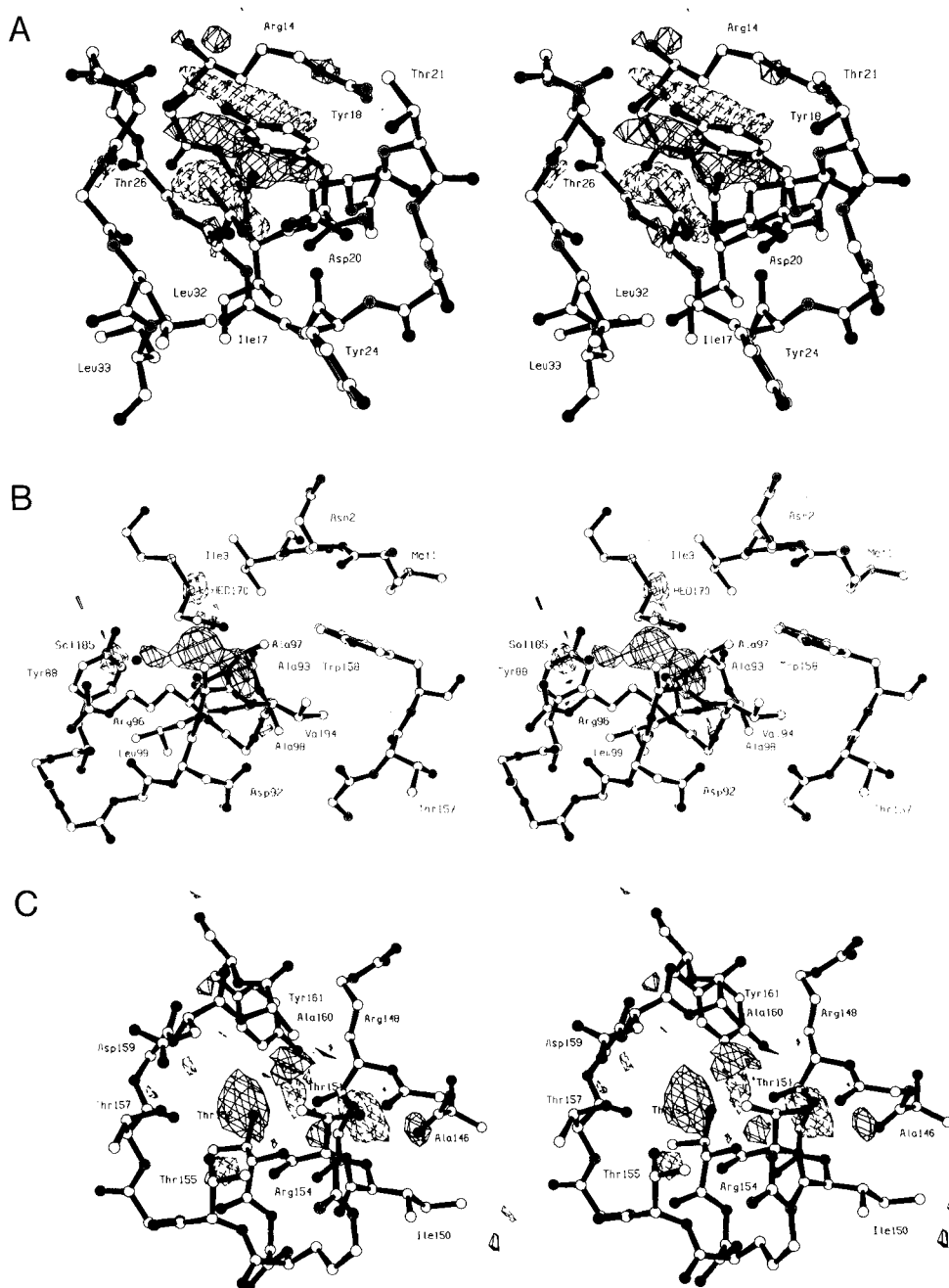


Fig. 1. Difference electron density maps. Coefficients ($F_{mut} - F_{WT^*}$), where the F -values are the observed structure amplitudes for the mutant and WT* crystals, respectively. Phase angles from the refined structure of WT*. Electron density contoured at 3.5σ (solid) and -3.5σ (broken), where σ is the average density throughout the unit cell. Oxygen atoms drawn solid, nitrogen atoms with radial spokes, and carbon atoms as open circles. **A:** Mutant T26S relative to WT*. **B:** Mutant A93T relative to WT*. Conventions as stated except that the electron density map is contoured at $\pm 4.0\sigma$. **C:** Mutant T151S relative to WT*.

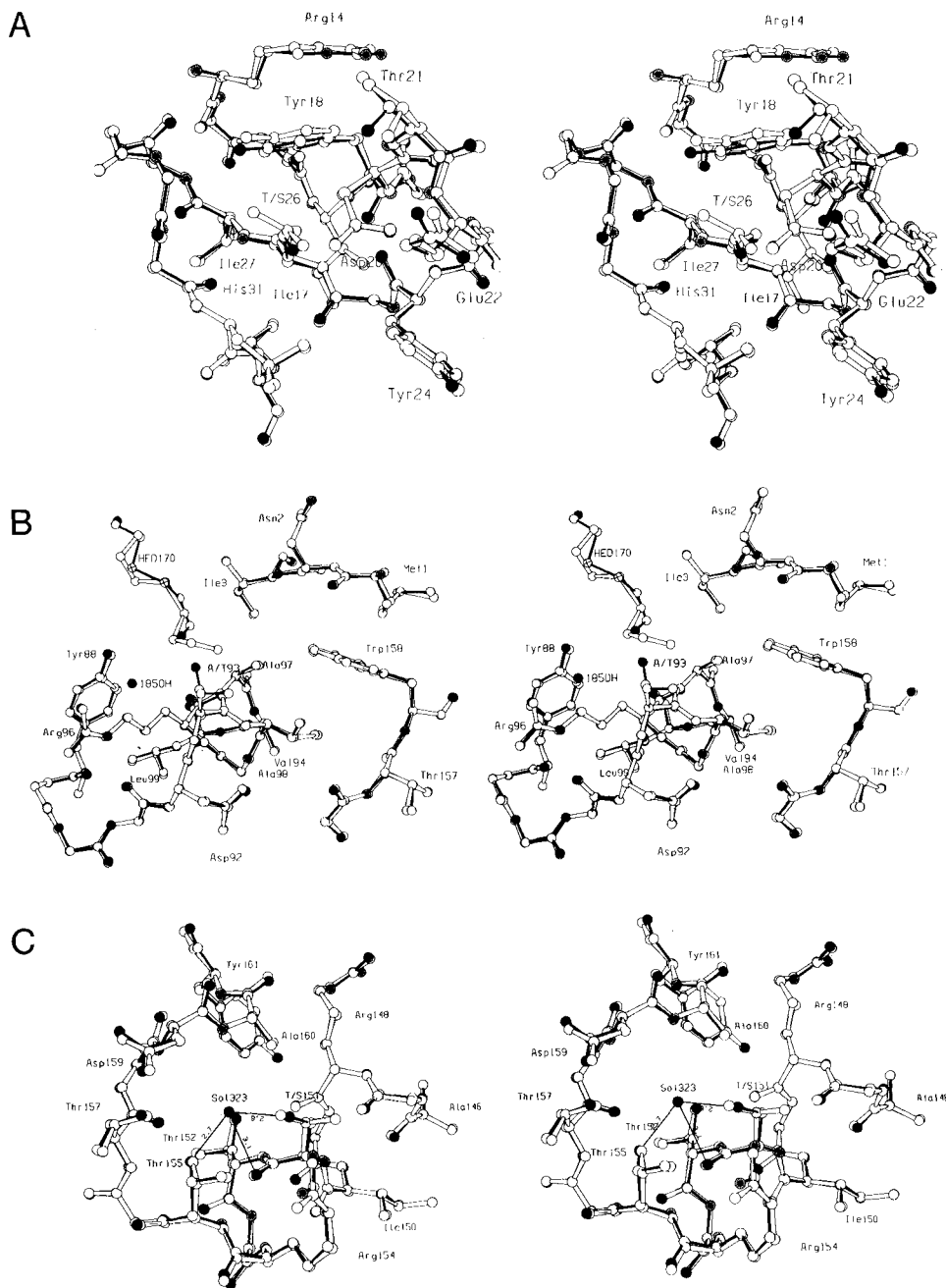


Fig. 2. Superpositions of refined mutant structures (open bonds) on WT* (solid bonds). In the mutant structures, oxygen atoms are drawn as solid circles, nitrogen atoms with radial spokes, and carbon atoms as open circles. **A:** Mutant T26S relative to WT*. **B:** Mutant A93T relative to WT*. **C:** Mutant T151S relative to WT*. Hydrogen bonds to solvent molecule Sol 323 are drawn as thin lines with the bond length in Ångstroms written next to the bond.

Ser 26 O γ brings with it the side chain of Asp 20. This in turn results in adjustments in Thr 21 and Glu 22. His 31 also moves slightly toward residue 26.

A93T

Figure 1B shows the difference density near the mutation site. Two positive peaks indicate the positions of the O γ^1 and C γ^2 atoms of Thr 93 in the mutant. In addition, two smaller positive and negative peaks indicate movement of the solvent molecule SOL 185. Another difference peak shows that a HEDS molecule (i.e., hydroxyethyl disulfide

or oxidized β -mercaptoethanol), adjacent to residue 93 in the wild-type crystal structure, has moved away from residue 93 to avoid a close contact with the newly introduced O γ^1 of Thr 93.

Figure 2B compares the final refined model of the mutant with the wild type. The side chain of Thr 93 adopts the *trans* conformation ($\chi_1 = -157^\circ$). There are virtually no changes in the structure, other than the introduction of the new side chain at the mutation site and the adjustment of SOL 185, which moves closer to residue 93 to make a 2.8-Å contact with Thr 93 O γ^1 and away from a contact with Arg 96 in the wild-type structure.

T151S

For this mutant (Fig. 1C) a large negative difference peak at the site of Thr 151 O γ^1 indicates that the hydroxyl of Ser 151 has rotated around the C $^\alpha$ -C $^\beta$ bond to occupy the position of the methyl group in the wild type. In addition, a large positive peak adjacent to Ser 151 O γ indicates a new solvent molecule bound to the mutant structure. Two other, smaller peaks suggest a second bound solvent molecule and the repositioning of another solvent molecule in the mutant structure.

Refinement (Fig. 2C) confirms that the hydroxyl of Ser 151 is positioned at the location of the methyl group of Thr 151 in wild type (in WT* $\chi_1 = -70^\circ$; in T151S $\chi_1 = 173^\circ$) and that a new solvent molecule, SOL 323, is coordinated by Thr 151 and Thr 155. It also shows that the mutant structure has changed very little relative to the wild type, with the exception of a slight motion of the side chain of Arg 154.

The most striking changes in this mutant involve the changes in solvent structure in the vicinity of substitution. As shown in Figure 3, new solvent molecules are added and "old" ones are rearranged. All of the changes can be related directly to the reorientation of the hydroxyl of residue 151. The bound solvent molecule (#323) is tightly coordinated by three protein ligands—Ser 151 O γ (2.6 Å), Ser 151 O (3.2 Å), and Thr 155 O γ^1 (2.7 Å)—as well as by two other solvent molecules—the preexisting SOL 175

(2.7 Å) and the new SOL 340 (3.0 Å). Together, these ligands provide almost perfect tetrahedral coordination. In addition, in the mutant, Ser 151 O γ possibly interacts with new solvent molecules #340 (3.6 Å) and #349 (3.3 Å). In the process of moving from its position in the wild-type structure, however, the hydroxyl of residue 151 loses hydrogen bonds it had with two other solvent molecules, #261 (3.0 Å) and #313 (3.1 Å). Despite this, the structural effect on these two solvent molecules is minimal. SOL 261 simply shortens its contact with the side chain of Arg 154, and SOL 313 with Lys 147 O. The separation between these two solvent molecules (2.8 Å) is virtually unchanged.

Other structural changes

Least-squares superpositions of the main-chain atoms of the three mutant structures onto the WT* structure show that there have been very few global changes. The root mean square (RMS) shifts are 0.14 Å (T26S), 0.12 Å (A93T), and 0.12 Å (T151S), all of which are close to the expected RMS error levels for the structures.

Nevertheless, in each case there are apparently changes in crystal contacts that result in conformational changes of a number of side chains in each mutant. Most of these are slight, involving small shifts. Larger changes are, however, indicated for Lys 16 (all three mutant structures), Asp 61 (T26S and A93T), Asp 72 (A93T, possibly due

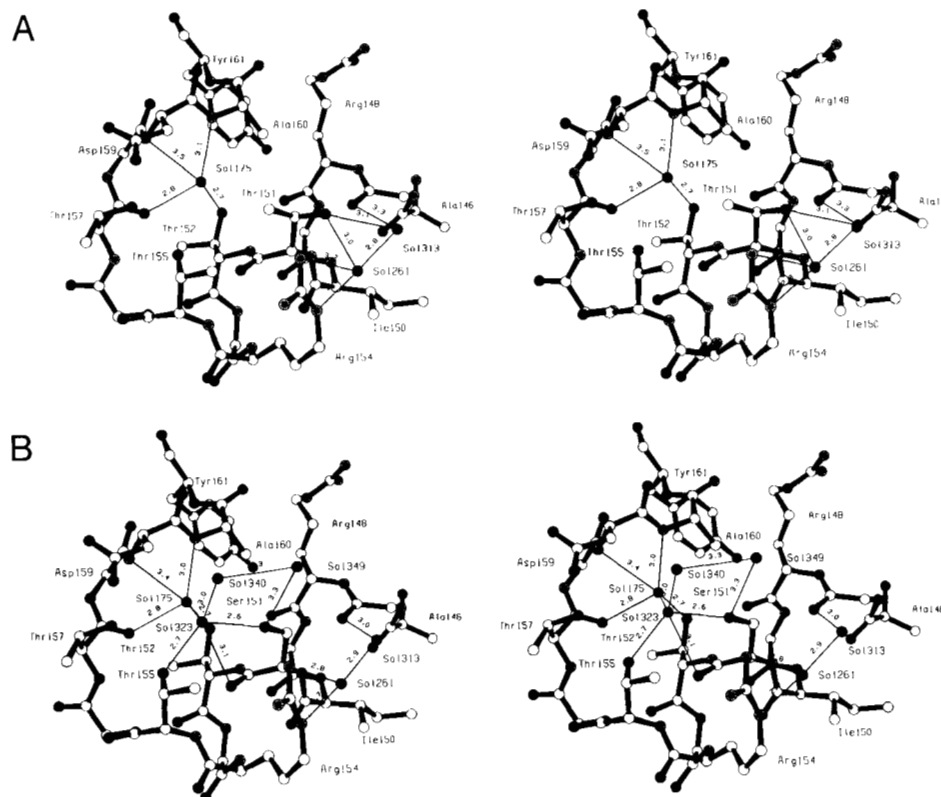


Fig. 3. Comparison of bound solvent in the vicinity of Thr 151 in WT* with bound solvent in the vicinity of Ser 151 in the mutant structure S151T. Oxygen atoms (including solvent) are drawn solid, nitrogen atoms with radial spokes, and carbon atoms as open circles. Hydrogen bonds are drawn as thin lines with the distance in Ångstroms listed next to the bond. **A:** WT* (Thr 151). **B:** Mutant (T151S).

to the shift of the HEDS molecule), Arg 76 (T26S and A93T), Arg 80 (T26S), Lys 83 (all three), Arg 119 (T151S), and Lys 162 (T26S). Five of these—Asp 61, Asp 72, Arg 76, Arg 80, and Lys 162—involve interactions with symmetry-related protein molecules in the crystal; the other three seem to be due to small changes within surrounding residues within the same molecule. Except for Asp 61 and Asp 72, all these side chains have relatively high thermal factors, indicating that they do not adopt a single well-defined conformation. In solution they may be to a large extent disordered.

One other change that also occurs at a crystal contact involves the bound HEDS molecule, which appears to shift ~ 2 Å in A93T. This occurs because the newly introduced side chain would otherwise produce an unfavorable van der Waals contact. As a consequence, the HEDS molecule in A93T would tend to overlap a symmetry-related copy of itself in the crystal, and presumably have partial occupancy in the alternative sites. The same is probably also true for the wild-type crystal form, as the HEDS O₁ and C₁ atoms here also tend to sterically clash across the twofold axis.

Discussion

The three mutants described in this paper illustrate the effect of the same type of mutation in three different structural contexts.

In the case of T26S, the structural changes that are seen suggest that it may be an example of stabilization due to the reduction of internal strain. The removal of the C^γ2 methyl group leads to a series of concerted movements (~ 0.2 – 0.5 Å) as surrounding residues relax into the resulting space. The shift of Tyr 18 is the largest and suggests that the apparent short contact of 2.9 Å between Thr 26 C^γ and Tyr 18 OH in the wild-type protein may be energetically unfavorable and is eliminated in the mutant.

In the case of A93T, the structural analysis is fully consistent with the observation that it has essentially the same stability as WT*. The side chain is fully exposed to solvent (Fig. 2B). Such a residue is expected to be equally solvated in the folded and unfolded forms, and substitutions at such a site are expected to have little if any effect on stability (unless they either affect the unfolded state or introduce new interactions in the folded protein). There is no evidence that the introduction of a threonine at site 93 modifies the protein structure, and we infer that it also does not modify the unfolded form. It might be noted that alanine is a helix-favoring residue and its introduction within α -helices can increase the stability of a protein (Zhang et al., 1991; Blaber et al., 1993). In the present case, however, residue 93 is at the Ncap + 1 position, not within the middle of the helix (Fig. 2B). Therefore, the present result is consistent with the idea that alanine is not especially helix-favoring if it is located at a site within the

first turn of the helix where the side chain is fully solvent exposed.

The mutant T151S is interesting in that its enhanced stability appears to be due to better hydrogen bonding in the mutant than in wild type. The result, however, would have been difficult to predict. In effect, the loss of the methyl group of residue Thr 151 “unplugs” a preformed solvent-binding site into which a water molecule can bind and allows the hydroxyl of Ser 151 to act as one of the ligands. The conformation of Thr 151 required to rotate its hydroxyl atom into this solvent-binding conformation would incur unacceptable close contacts between the γ -carbon and residues 147, 148, and 160. In the wild-type conformation, however, the γ -methyl of Thr 151 blocks the solvent-binding site by creating an unacceptable van der Waals contact.

The newly bound water molecule in the mutant structure is coordinated by a number of hydrogen bonds, four of which appear to be in an approximately tetrahedral arrangement (Fig. 3B). Also the water molecule enhances the interactions of the solvent molecule (SOL 175) that is already bound to the protein. The mutation results in an extended interwoven network of hydrogen bonds including both protein and bound solvent (Fig. 3B). No doubt these multiple interactions contribute to the observed stabilization. Because the multiple hydrogen-bonding requirements of the protein atoms and bound solvent are satisfied simultaneously, it distributes the entropy cost of localizing both the solvent and the protein.

Several other examples of Thr \rightarrow Ser and Ala \rightarrow Thr mutations in T4 lysozyme have been identified. These include T59S (Bell et al., 1992), T152S (Alber et al., 1987a; Dao-pin et al., 1991), T157S (Alber et al., 1987b), A98T (Alber et al., 1987a), A146T (Alber et al., 1986), and A160T (Alber et al., 1987a). All appear to be temperature-sensitive to a greater or lesser degree, showing that there is no reason to believe that threonine to serine (or alanine to threonine) substitutions are intrinsically stabilizing.

Conclusions

As has been shown many times before, the effect of a mutation on the structure and stability of a protein is strongly dependent upon the structural context in which it occurs. In the case of the two stabilizing mutations, T26S and T151S, both the structural consequences and the manner in which they appear to achieve their stabilizing effects are different: the former, by removing an unfavorable packing interaction in the N-terminal domain of the protein; the latter, by unblocking a latent solvent-binding site in the C-terminal domain. The neutral mutation, A93T, is solvent exposed and has no effect on either structure or stability.

The results support the expectation that there is a cause-and-effect relationship between structure and stability. In both T26S and T151S, although the effects on the struc-

ture are seen to be quite different, the structural changes can be interpreted in terms of enhanced stability of the folded protein. Conversely, A93T has no apparent effect on the structure of the protein. This observation is encouraging in terms of the use of known protein structures as a basis for rational improvement of stability.

The results also illustrate how random mutagenesis can be used to obtain proteins with a desired change in phenotype, in this case enhanced thermostability. Although the reasons for enhanced stability can be rationalized in terms of the observed structural changes, it would have been very difficult to predict, in advance, that these mutants would be stabilizing.

Materials and methods

The reference protein is the cysteine-free variant of bacteriophage T4 lysozyme containing the mutations Cys 54 → Thr and Cys 97 → Ala, referred to as WT* (Matsumura & Matthews, 1989).

Mutants were obtained using an M13-based mutagenesis and screening system developed to identify thermostable variants of T4 lysozyme (Pjura et al., 1993).

Crystals suitable for crystallographic analysis were obtained by macroseeding. Seed crystals were grown by combining 2–5 μ L of a 15–20-mg/mL solution of the protein in SP buffer (0.1 M Na/K PO₄, 0.55 M NaCl, 0.02% NaN₃, pH 6.5) with an equal volume of 2 M Na/K PO₄, 0.4% HEDS, pH 6.8, on silanized glass coverslips. These were sealed over 0.5 mL of 2 M Na/K PO₄, pH 6.8, in wells of a Linbro plate, using Vaseline, and stored at 5 °C. Trigonal crystals, typically 0.05–0.10 mm on a side, grew in 1–2 weeks and were used as seeds. The seed crystals were washed by transferring them to a 50- μ L drop of 0.8 M Na/K PO₄, pH 6.8, and equilibrating them for 4 h, all at 5 °C. Seeding drops were made by transferring a single washed crystal to a drop containing 4 μ L of the same protein in SP buffer and 4 μ L of 2 M Na/K PO₄, 0.4% HEDS, pH 6.8, in a spot of a Linbro microdepression dish, and sealing with 0.5 mL of 2 M Na/K PO₄, pH 6.8, in the well using a coverslip and Vaseline. In successful drops, no additional nucleations occurred and it was possible to grow perfect single crystals, up to 0.5 mm on a side, from the seeds in 2–3 weeks.

Crystals used for data collection were equilibrated before mounting by gradual addition of a total of 42 μ L of 2.3 M buffer (1.05 M K₂HPO₄, 1.26 M NaH₂PO₄, 0.23 M NaCl, 1.4 mM 2-mercaptoethanol, pH 6.7). Data were collected on a Xuong-Hamlin Mark II multiwire area detector, using omega-scan oscillation sweeps. Statistics for the three data sets are listed in Table 2.

The structure of the WT* protein was used as the starting model for the respective refinements. Both $2F_o - F_c$ and $F_{\text{mutant}} - F_{\text{WT*}}$ maps, phased using the WT* coordinates, were examined with the molecular model-building

Table 2. Crystallographic data^a

	WT*	T26S	A93T	T151S
Data collection				
Total observations	—	54,414	49,980	50,320
Independent reflections	14,345	20,529	17,845	20,832
R_{merge}	4.6%	4.5%	4.8%	4.5%
a (Å)	60.9	60.9	61.0	61.0
b (Å)	60.9	60.9	61.0	61.0
c (Å)	96.8	96.8	97.0	96.8
R_{isom} (20–1.7 Å)	—	15.6%	12.1%	12.2%
Refinement				
Final R -factor	14.8%	15.8%	16.5%	16.4%
$\Delta_{\text{bond length}}$ (Å)	0.015	0.016	0.017	0.018
$\Delta_{\text{bond angle}}$ (°)	2.1	2.5	2.7	2.6
$\Delta_{\text{nonbonded contacts}}$ (Å)	—	0.024	0.033	0.031
Reflections included	14,562	18,272	17,806	20,810
Resolution (Å)	1.75	20–1.7	20–1.7	20–1.7
Data completeness (%)	65	75	73	85

^a R_{merge} gives the agreement between independent measurements of the same intensity value; a , b , and c are the unit cell dimensions; R_{isom} gives the average difference between structure amplitudes measured for WT* and those for the mutant; $\Delta_{\text{bond length}}$, $\Delta_{\text{bond angle}}$, and $\Delta_{\text{nonbonded contacts}}$ give the average differences between the bond lengths, bond angles, and nonbonded contacts in the final refined model and those expected for "ideal" stereochemistry.

program FRODO (Jones, 1982), and changes were made as appropriate at the mutation sites. The models were then subjected to alternating rounds of restrained least-squares positional and temperature-factor refinement, using the TNT refinement package (Tronrud et al., 1987), and additional model-building sessions with FRODO, until their R -factors had converged and no additional changes could be made in the models. Refinement statistics for the three final models are shown in Table 2.

Acknowledgments

We are most grateful to Sheila Pepiot and Joan Wozniak for protein purification, Larry Weaver for assistance with X-ray data collection, and Elisabeth Eriksson for advice on crystal seeding. This work was supported in part by a PHS fellowship (GM11836) to P.P., by a grant from the NIH (GM21967) to B.W.M., and by the Lucille P. Markey Charitable Trust.

References

- Alber, T., Dao-pin, S., Nye, J.A., Muchmore, D.C., & Matthews, B.W. (1987a). Temperature-sensitive mutations of bacteriophage T4 lysozyme occur at sites with low mobility and low solvent accessibility in the folded protein. *Biochemistry* 26, 3754–3758.
- Alber, T., Dao-pin, S., Wilson, K., Wozniak, J.A., Cook, S.P., & Matthews, B.W. (1987b). Contributions of hydrogen bonds of threonine 157 to the thermodynamic stability of phage T4 lysozyme. *Nature* 330, 41–46.
- Alber, T., Grütter, M.G., Gray, T.M., Wozniak, J., Weaver, L.H., Chen, B.-L., Baker, E.N., & Matthews, B.W. (1986). Structure and stability of mutant lysozymes from bacteriophage T4. *UCLA Symp. Mol. Cell. Biol.*, n.s. 39, 307–318.

- Bell, J.A., Becktel, W.J., Sauer, U., Baase, W.A., & Matthews, B.W. (1992). Dissection of helix capping in T4 lysozyme by structural and thermodynamic analysis of six amino acid substitutions at Thr 59. *Biochemistry* 31, 3591–3596.
- Blaber, M., Zhang, X.-J., & Matthews, B.W. (1993). Structural basis of amino acid α -helix propensity. *Science* 260, 1637–1640.
- Dao-pin, S., Alber, T., Baase, W.A., Wozniak, J.A., & Matthews, B.W. (1991). Structural and thermodynamic analysis of the packing of two α -helices in bacteriophage T4 lysozyme. *J. Mol. Biol.* 221, 647–667.
- Jones, T.A. (1982). FRODO: A graphics fitting program for macromolecules. In *Computational Crystallography* (Sayre, D., Ed.), pp. 303–317. Oxford University Press, Oxford, UK.
- Matsumura, M., Becktel, W.J., Levitt, M., & Matthews, B.W. (1989). Stabilization of phage T4 lysozyme by engineered disulfide bonds. *Proc. Natl. Acad. Sci. USA* 86, 6562–6566.
- Matsumura, M. & Matthews, B.W. (1989). Control of enzyme activity by an engineered disulfide bond. *Science* 243, 792–794.
- Matthews, B.W. (1987). Genetic and structural analysis of the protein stability problem. *Biochemistry* 26, 6885–6888.
- Matthews, B.W. (1993). Structural and genetic analysis of protein stability. *Annu. Rev. Biochem.* 62, 139–160.
- Matthews, B.W., Nicholson, H., & Becktel, W.J. (1987). Enhanced protein thermostability from site-directed mutations that decrease the entropy of unfolding. *Proc. Natl. Acad. Sci. USA* 84, 6663–6667.
- Nicholson, H., Anderson, D.E., Dao-pin, S., & Matthews, B.W. (1991). Analysis of the interaction between charged side-chains and the α -helix dipole using designed thermostable mutants of phage T4 lysozyme. *Biochemistry* 30, 9816–9828.
- Pjura, P., Matsumura, M., Baase, W.A., & Matthews, B.W. (1993). Development of an in vivo method to identify mutants of phage T4 lysozyme of enhanced thermostability. *Protein Sci.* 2, 2217–2225.
- Tronrud, D.E., Ten Eyck, L.F., & Matthews, B.W. (1987). An efficient general-purpose least-squares refinement program for macromolecular structures. *Acta Crystallogr.* A43, 489–503.
- Zhang, X.-J., Baase, W.A., & Matthews, B.W. (1991). Toward a simplification of the protein folding problem: A stabilizing polyaniline α -helix engineered in T4 lysozyme. *Biochemistry* 30, 2012–2017.